JOURNAL OF AGRICULTURAL AND FOOD CHEMISTRY
ARTICLE

J. Agric. Food Chem. 2010, 58, 1679–1684 1679
DOI:10.1021/jf903308u

A Novel Method To Quantify the Adulteration of Extra Virgin Olive Oil with Low-Grade Olive Oils by UV−Vis

José S. Torrecilla,* Ester Rojo, Juan C. Domínguez, and Francisco Rodríguez

Department of Chemical Engineering, Faculty of Chemistry, University Complutense of Madrid, 28040 Madrid, Spain

A simple and novel method to quantify adulterations of extra virgin olive oil (EVOO) with refined olive oil (ROO) and refined olive−pomace oil (ROPO) is described here. This method consists of calculating chaotic parameters (Lyapunov exponent, autocorrelation coefficients, and two fractal dimensions, CPs) from UV−vis scans of adulterated EVOO samples. These parameters have been successfully linearly correlated with the ROO or ROPO concentrations in 396 EVOO adulterated samples. By an external validation process, when the adulterating agent concentration is less than 10%, the integrated CPs/UV−vis model estimates the adulterant agent concentration with a mean correlation coefficient (estimated versus real concentration of low grade olive oil) greater than 0.97 and a mean square error of less than 1%. In light of these results, this detector is suitable not only to detect adulterations but also to measure impurities when, for instance, a higher grade olive oil is transferred to another storage tank in which lower grade olive oil was stored that had not been adequately cleaned.

KEYWORDS: Lyapunov exponent; autocorrelation function; fractal dimension; UV−vis; adulteration; olive oils

INTRODUCTION

The most important requirement of consumers is to have the highest quality in all bought goods. This requisite is even more obligatory when the products present health implications for consumers. Regretfully, in the food sector, we are still faced with the problem of adulteration. A deplorable example of this is the case of edible rapeseed oil with aniline-based compounds (commonly called Spanish toxic oil syndrome). This adulteration caused serious illness and continues to affect more than 20 000 people, some of whom have died (*1*).

Given that extra virgin olive oil (EVOO) is the only edible oil which comes directly from the juice of fruits (the olive), EVOO is one of the most valuable oils in the world. Because of this, the adulteration in the edible oil sector is mainly focused on EVOO. The adulteration is habitually carried out by blending EVOO with low-grade olive oils (olive−pomace oil or refined olive oil) or with seed oils (*2*−*4*). The detection and quantification of adulterant oil concentration depends on the adulterated compound concentration and the physicochemical similarity between it and EVOO (*1*−*3*, *5*).

Although there is no single analytical method to determine the adulteration (*6*), in order to fight against these fraudulent activities, physicochemical properties (density, refractive index, etc.) and/or key compound concentrations (polyphenols, acids, sterols, etc.) in the EVOO must be measured (*7*, *8*). The composition of oleic samples can be determined using technical analyses such as nuclear magnetic resonance spectroscopy (*9*), Fourier transform Raman spectroscopy (*10*), fluorescence spectroscopy, high-performance liquid chromatography (*11*−*12*), UV−vis spectroscopy (*13*, *14*), etc.

Once the information has been taken from the analytical equipment, powerful statistical techniques are usually applied to extract the relevant information (**Figure 1**). Depending on the requirement of the analyses and the nature of the information, these data can be analyzed by techniques based on linear (principal component analysis, multivariable regression techniques, etc.) or nonlinear algorithms in more complex situations (*1*−*4*, *9*).

Due to the fact that the adulteration of olive oil not only is an economic fraud but also can be damaging to health, a reliable, fast, simple, and cheap method to detect these undesirable compounds is required. Currently, chemometric tools based on nonlinear algorithms present the most successful results (*5*, *15*). As tools based on chaotic parameters (CPs) can detect slight variations in initial experimental conditions (*16*), models based on CPs could be adequate to determine the adulteration with only small concentrations of low-grade olive oils. For these reasons and with the goal of finding the simplest (easiest chemical and mathematical performance) model, linear algorithms based on chaotic parameters have been tested here.

In the chemical field, these types of chaotic models have only been successfully applied by researchers. Among others, it has been applied to the modelization of simple microbial systems consisting of two microbial populations competing for a single nutrient (*17*). Also, Torrecilla et al. determined noisy signals from UV spectrophotometer, thermogravimetric analyzer (TGA), and differential scanning calorimeter (DSC) apparatus in the ionic

*To whom correspondence should be addressed. Fax: +34 91 394 42 43. Tel: +34 91 394 42 40. E-mail: jstorre@quim.ucm.es.

Published on Web 01/13/2010

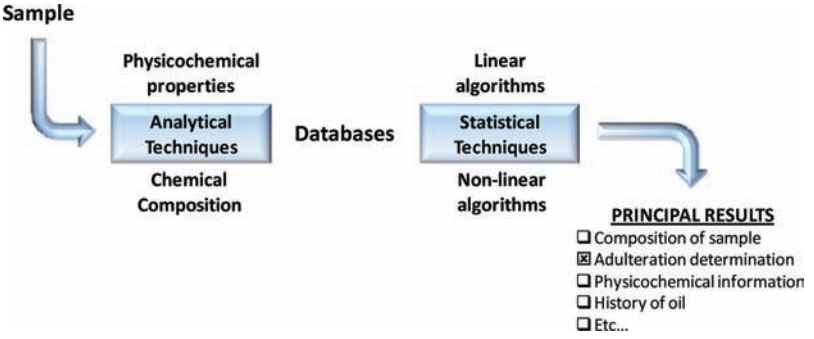

Figure 1. General scheme to detect/determine lack of quality.

Table 1. Botanical Origin, Brand, and Number of Oil Samples Used

type of olive oil	no. of samples	brand
extra virgin olive oil	396	Aceites Borges Pont SAU
refined olive oil	189	KOIPE, SOS Cuétara SA
refined olive−pomace oil	189	DIA

liquid field (*16*). To the best of our knowledge, in the edible oil field, there are no models based on chaotic parameters. Given the successful results achieved in other scientific fields, a model based on chaotic parameters has been applied to quantify the adulteration of EVOO with refined olive oil or refined olive−pomace oil by chaotic parameters and regression models using UV−vis scans of adulterated samples. Once the model was optimized, it was tested to detect adulteration with refined olive oil and refined olive−pomace oil.

MATERIALS AND METHODS

Instrumentation and Oil Samples. A Varian Cary 1E UV−visible spectrophotometer was employed for absorbance measurements using quartz cells of 1 cm path length. All stock solutions were prepared using an AG 245 Mettler Toledo analytical balance (precision 0.01 mg).

The botanical origin and quality of all samples of extra virgin olive oil were guaranteed by the supplier (**Table 1**). In addition, samples of refined olive oil (ROO) and refined olive−pomace oil (ROPO) were provided by Spanish companies, which are shown in **Table 1**. All were stored in the dark at room temperature until the day of analysis. To estimate and detect the adulteration of EVOO with other low-cost olive oils, mixtures containing EVOO and refined olive oil or refined olive−pomace oil were prepared. Following the procedure shown in the Official Journal of the European Union (Commission Regulation (EC) No 640/2008, Annex IX), all the samples were prepared and diluted in isooctane (C_8H_{18} ≥99.5% purity, from Merck).

Chaotic Parameters Used. To detect other low-grade olive oils in the EVOO several chaotic parameters (Lyapunov exponent, autocorrelation functions, and fractal dimensions) have been calculated by UV−vis scans of adulterated EVOO samples.

Lyapunov Exponents. Lyapunov exponents (LEs) are always real numbers and provide additional useful information about the system studied (*18*). These exponents characterize the dynamics of a complex process and quantify the average growth of infinitesimally small errors at initial points. LE values characterize the rate of separation of infinitesimally close trajectories. This can be used to measure the sensitivity of a system's behavior to initial conditions (*19*). The LE parameter has been calculated by following eq **1**.

$$\mathrm{LE} = \frac{1}{\Delta\lambda_m}\sum_{k=1}^{m}\log_2\frac{L(\lambda_k)}{L(\lambda_{k-1})} \quad (1)$$

where $\Delta\lambda_m$, k and $L(\lambda_k)$ are the prediction wavelength interval, the wavelength, and the Euclidean distance between the developed points in the space, respectively. For instance, considering p_1 at (λ_{k-1}, Absorbance$_{k-1}$) and p_2 at (λ_k, Absorbance$_k$), the Euclidean distance between p_1 and p_2 ($L(\lambda_{k-1})$) is $[(\lambda_{k-1} - \lambda_k)^2 + (\mathrm{Absorbance}_{k-1} - \mathrm{Absorbance}_k)^2]^{1/2}$. Detailed information can be found elsewhere (*18*, *19*). This parameter is one of the most sensitive in determining the chaotic dynamics of processes (*18*). Depending on the sign of the maximal LE (MLE), different types of attractors (dynamic systems evolve after a long period of time) can be found. MLE < 0 represents stable fixed, MLE = 0 or MLE = ∞ implies stable limit cycle or noise, respectively, and 0 < MLE < ∞ implies chaos, which means that neighboring points of trajectories in the space diverge (*20*).

Autocorrelation Functions ($R_{\Delta\lambda}$). These parameters measure linearly how strongly on average each data point is correlated with wavelength lag ($\Delta\lambda$) (eq **2**) (*20*). These are the ratio of the autocovariance to the variance of the data. In general, $R_{\Delta\lambda}$ is between 1 (small k) and 0 (large k) (*18*)

$$R_{\Delta\lambda} = \frac{\sum_{n=1}^{N-k}(X_n - \bar{X})(X_{n-k} - \bar{X})}{\sqrt{\sum_{n=1}^{N-k}(X_n - \bar{X})^2 \sum_{n=1}^{N-k}(X_{n-k} - \bar{X})^2}} \quad (2)$$

where X, $\bar{X}$ and N represent the absorbance set of the measurements by UV−vis spectrophotometry, their average, and the total number of data sets, respectively. Given that the $\Delta\lambda$ value ranges between 0 and 650 nm with $\Delta\lambda$ = 50 nm (14 parameters) (*18*, *19*), in the case of k = 50 nm (in time data series, k is commonly called lag time), throughout the work $R_{\Delta\lambda}$ values are referred to as R_{50}.

Fractal Dimensions. The dimensions of a line, plane, and volume are well-known. When the image is not exactly one of the aforementioned, the calculation of its dimension is more difficult, and this even more so when the dimension of a fractal image is required. In these cases, this dimension can be calculated by eq **3**

$$\text{fractal dimension} = \frac{\log P}{\log M} \quad (3)$$

where P and M are the number of subspaces into which the initial area can be divided and the magnified factor, respectively. For instance, the Sierpinski triangle fractal dimension is 1.584 (P = 3 and M = 2). When the fractal dimension of experimental curves is required, its calculation becomes more complex. In these cases, the fractal dimensions quantitatively describe how an object fills its space (*21*). In general, these fractal dimensions are real numbers that quantitatively describe how an object fills its space. In plane geometry, objects are solid and continuous, and given that they have no holes, they have integer dimensions. Fractals are rough and often discontinuous, and so they present noninteger dimensions. From a fractal geometry point of view, the fractal dimension is a measure of complexity that is used to describe the irregular nature of lines, curves, planes, or volumes. In this work, the regularization dimension (RD) and the box dimension (BD) using the plain box method have been computed by Fraclab version 2.0 (Toolbox of Matlab version 7.01.24704, R14) (*22*). Considering the original signal as fractal, its graph will have an infinite length. Taking into account RD and the fact that all regularized versions have a finite length, the RD measures the speed at which this convergence to the infinite takes place. To calculate BD, the software works exactly in the same way as when it computes the regularization dimension, except that in this case different box sizes are tested. In almost all cases, the estimation of fractal dimension by the box method is less accurate than the calculation by the regularization method. All necessary

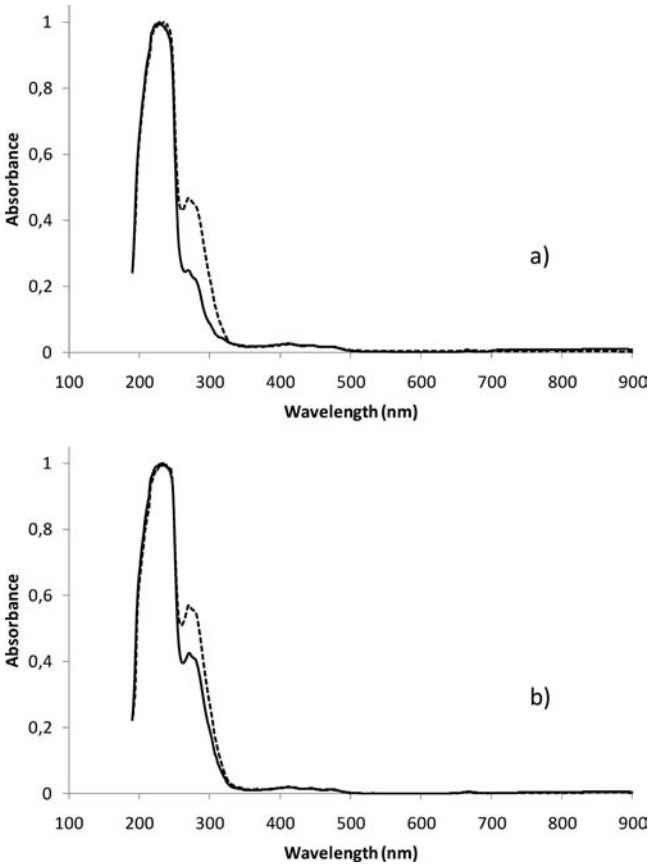

Figure 2. UV−vis scans of mixtures composed of extra virgin olive oil and (a) ROO (—, 0.882%; - - -, 4.819% or (b) ROPO (—, 0.834%; - - -, 4.562%).

parameter values to calculate RD and BD were selected by default configuration settings of the software used (*22*).

Learning, Verification, and Validation Samples. Every data set of the learning and verification samples is composed of 17 aforementioned chaotic parameters (14 autocorrelation parameters, 1 Lyapunov exponent, and 2 fractal dimensions) with their respective concentrations of low-grade olive oil in percent (ROO and ROPO). These parameters were calculated from the UV−vis scans from all binary mixtures composed of EVOO, ROO (0−10% w/w), or ROPO (0−10% w/w). As an example, UV−vis scans of adulterated samples composed of EVOO and ROO (0.9 and 5% w/w) and ROPO (0.8 and 5% w/w) are shown in **Figure 2**. For each concentration, three different solutions were made and each mixture was scanned three times. The mean of the three concentration values of refined olive oil and refined olive pomace oil in extra virgin olive oil is shown in two tables in **Figure 3**. Although the EVOO samples are adulterated with ROO and ROPO, as can be seen, both profiles with similar concentration values are similar. The learning and verification samples are composed of 378 data sets, which were distributed into 189 for EVOO + ROO and 189 for EVOO + ROPO. The only difference between the verification and learning samples is that the latter is composed of 80% (302 data sets) of data and the former of the remaining 20%. Taking into account that every datum of the verification sample should be interpolated within the learning range, the data were randomly distributed between both samples (*23*).

On the other hand, with relation to the external validation process, the aforementioned chaotic parameters have been calculated using different UV−vis scans from binary mixtures composed of EVOO and ROO or ROPO. Using these chaotic parameters and their respective adulterating oil concentrations, an external validation sample has been made. It is composed of the results achieved using low-grade olive oils. This external validation sample presents the same format as the learning and verification samples (*23*).

Linear Models. The linear models tested in this work are considered linear in the parameters, also called statistically linear (*24*). Linear and multiple linear regressions are the most widely used and known modeling methods. They have been adapted to a broad range of situations. In a

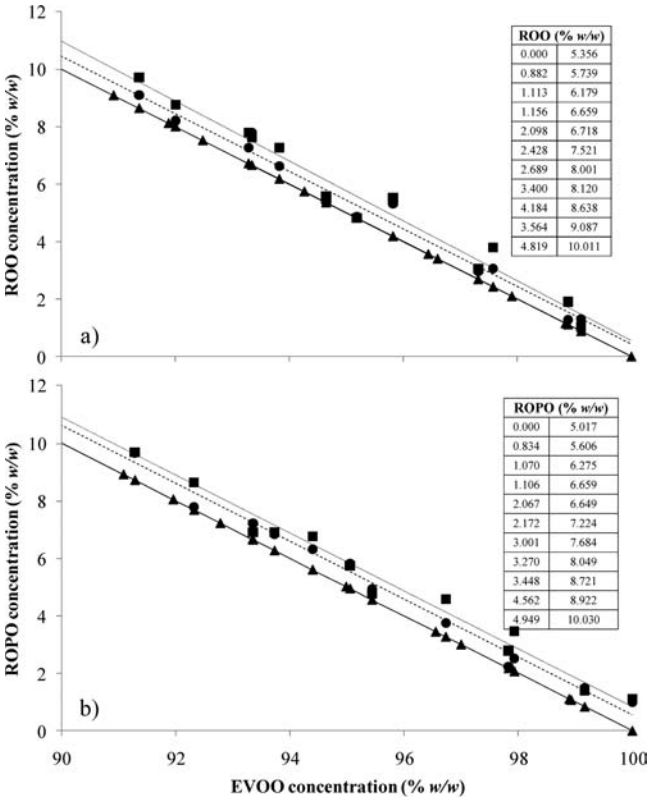

Figure 3. Mean of three experimental concentration values of refined olive oil (ROO) and refined olive−pomace oil (ROPO) (in tables) and their estimations using eqs **5**−**7** in the verification process: (a) UV−vis concentrations of ROO/EVOO mixtures (−▲−)and ROO concentrations estimated by eqs **5 and 7** and their respective linear correlations (■, ●, · · ·, and - - -, respectively); (b) UV−vis concentrations of ROPO/EVOO mixtures (−▲−) and ROPO concentrations estimated by eqs **6 and 7** and their respective linear correlations (■, ●, · · ·, and - - -, respectively).

multivariate case, when there is more than one independent variable, the regression line cannot be visualized in two-dimensional spaces. In this case, a linear equation containing all those variables can be constructed (eq **4**)

$$y = \alpha_0 + \sum_{i=1}^{n} \alpha_i x_i + \varepsilon \quad (4)$$

where y, n, α_i (α_0, α_1, ..., α_n), x_i (i = 1, 2, ..., n), and ε represent response variables (adulterating concentration), number of observations, parameters of the model, independent variables (chaotic parameters), and random error, respectively (*25*). The error term is an unobservable random variable that represents the residual variation and will be assumed to have zero mean, constant variance, and a normal distribution. The linear models are not limited to lines or planes but include a fairly wide range of shapes (*24*). Due to its simplicity (eq **4**), this type of linear model has been used here. The linear models and statistical analyses were carried out by SPSS version 15.0.1.

RESULTS AND DISCUSSION

A database formed by quantity of low-grade olive oil, Lyapunov exponent, autocorrelation coefficients (14 parameters), and two fractal dimensions was made (vide supra). In the first study, the adulteration of EVOO with refined olive oil and refined olive−pomade oil was individually investigated. Then, a global model to estimate the adulteration with low-grade olive oil was proposed. Finally, the global model was externally validated using two external validation samples (*23*). Given that the chaotic parameters are defined for specific initial experimental conditions, every equation is only adequate in the detection of the adulterated oils for which it has been established.

Table 2. Estimation of ROO as Adulterating Agent of EVOO by Linear Regression Models

α_0	α_1	α_2	α_3	α_4	α_5	α_6	R^{2a}	MSE[a]
121.845	$-101.734 \cdot RD$						0.589	3.424
-28.844	$-27.774 \cdot R_0$	$66.436 \cdot BD$					0.831	1.485
-23.353	$-43.100 \cdot R_{200}$	$7.150 \cdot 10^6$ LE	$61.024 \cdot BD$				0.874	1.170
88.741	$-52.827 \cdot R_{200}$	$-16.835 \cdot R_{600}$	$-64.809 \cdot RD$	$36.728 \cdot BD$			0.913	0.860
53.125	$281.152 \cdot R_{200}$	$354.967 \cdot R_{300}$	$-502.236 \cdot R_{350}$	$46.340 \cdot R_{450}$	$-98.092 \cdot RD$		0.944	0.591
33.011	$221.437 \cdot R_{200}$	$286.566 \cdot R_{300}$	$-405.294 \cdot R_{350}$	$33.356 \cdot R_{450}$	$-79.364 \cdot RD$	$18.613 \cdot BD$	0.951	0.557

[a] $[\mathrm{ROO}] = \sum_{i=0}^{6} \alpha_i$.

Table 3. Estimation of ROPO as Adulterating Agent of EVOO by Linear Regression Models

α_0	α_1	α_2	α_3	α_4	α_5	α_6	R^{2a}	MSE[a]
119.780	$-100.559 \cdot RD$						0.874	1.017
80.231	$-398.908 \cdot R_{50}$	$214.519 \cdot R_{550}$					0.911	0.762
119.176	$37.804 \cdot R_{250}$	$38.110 \cdot R_{650}$	$-112.208 \cdot RD$				0.938	0.561
85.776	$107.317 \cdot R_{450}$	$-113.251 \cdot R_{500}$	$93.715 \cdot R_{550}$	$-79.752 \cdot RD$			0.969	0.300
112.649	$-271.189 \cdot R_0$	$-371.456 \cdot R_{100}$	$147.851 \cdot R_{150}$	$307.899 \cdot R_{550}$	$-1.354 \cdot 10^7 \cdot LE$		0.981	0.195
172.702	$-237.429 \cdot R_0$	$-210.998 \cdot R_{100}$	$122.129 \cdot R_{450}$	$218.537 \cdot R_{550}$	$-1.248 \cdot 10^7 \cdot LE$	$-43.862 \cdot RD$	0.990	0.110

[a] $[\mathrm{ROPO}] = \sum_{i=0}^{6} \alpha_i$.

Adulteration of EVOO with ROO. In order to determine the most suitable model to estimate the concentration of refined olive oil (dependent variable) and as a consequence of the combination of the aforementioned 17 chaotic parameters (independent variables), 131 072 models were designed. Here, 6 models with the best statistical results using 6 respective groups formed by 1−6 independent variables and their statistical results are shown in **Table 2**. As expected, the models, which use more independent variables, can better explain the response surface. Thus, the statistical results improved when more independent variables were used (**Table 2**). As there are nearly 30 data sets (189/7) for each parameter to be optimized, the 6-order model can be reliably used. It might be worth mentioning that, in all proposed models to estimate the ROO concentration, at least one fractal dimension is used.

Although the aforementioned models can be used to easily determine the adulteration of EVOO with ROO, in order to find the most reliable model using the 17 independent variables, the model with the best statistical results formed by 10 variables has been selected (eq **5**; $R^2 > 0.980$, MSE < 0.312). As can be seen, there are nine independent variables related to the autocorrelation functions and a fractal dimension. Although in this model the Lyapunov exponent is not used, it is used in other models with statistical slightly poorer results (**Table 2**).

$$[\mathrm{ROO}] = 140.998 - 791.609 \cdot R_{50} + 656.991 \cdot R_{100} - 554.949 \cdot R_{150} + 815.393 \cdot R_{200} + 961.940 \cdot R_{300} - 1203.130 \cdot R_{350} + 401.341 \cdot R_{450} + 282.176 \cdot R_{500} + 40.927 \cdot R_{600} - 95.083 \cdot \mathrm{RD} \quad (5)$$

Different combinations of all chaotic parameters presented here can suitably quantify the ROO concentration as an adulterating agent of EVOO when the former concentration is less than 10%. To sum up, the UV−visible scans of oil sample (EVOO + ROO) and the chaotic parameters calculated from them can detect and determine the adulterating agent concentrations using a simple method. Nevertheless, better statistical results can be achieved establishing nonlinear models between the aforementioned chaotic parameters and ROO concentrations, but the model, and thus its calculation procedure, is more complex. The estimated concentrations of ROO using eq **5** are compared with their respective UV−vis concentrations in **Figure 3**.

Adulteration of EVOO with ROPO. To detect/quantify the concentration of ROPO as an adulterating agent in EVOO samples by the aforementioned mathematical procedure, 131 072 linear regression models have been defined. The six most suitable model using groups formed by 1−6 independent variables and their statistical results are shown in **Table 3**. It is worth pointing out that only RD-independent variables can linearly describe the concentration of ROPO ($R^2 > 0.87$, MSE < 1.017). In addition, different combinations of all other chaotic parameters presented here can more adequately quantify the adulterating agent of EVOO when the ROPO concentration is less than 10%. A comparison of **Tables 2** and **3** shows that linear models based on the chaotic parameters studied can better quantify the ROPO than they can ROO as an adulterating agent of EVOO.

Although the aforementioned models can be used easily and reliably to determine the adulteration of EVOO with ROPO, the regression model with the best statistical results using 10 independent variables is shown in eq **6** ($R^2 > 0.997$, MSE < 0.035). More independent variables could be used to make a linear model, but the statistical results did not improve sufficiently (R^2 from 0.998 to 0.999 and the MSE from 0.035 to 0.023) to justify this step.

$$[\mathrm{ROPO}] = -385.729 - 810.572 \cdot R_0 + 1407.840 \cdot R_{50} - 2361.780 \cdot R_{100} + 122.416 \cdot R_{150} + 826.248 \cdot R_{200} - 566.804 \cdot R_{250} + 833.950 \cdot R_{300} - 209.442 \cdot R_{350} - 1.197 \cdot 10^7 \cdot \mathrm{LE} + 7.214 \cdot \mathrm{BD} \quad (6)$$

To sum up, simple linear regression models designed by the chaotic parameters calculated from the UV−vis scans of adulterated oil samples can accurately detect/determine the adulterating agent concentration. The estimated concentrations of ROPO using eq **6** are compared with their respective UV−vis concentrations in **Figure 3**.

Adulteration of EVOO with ROO and ROPO. Bearing in mind that the type of adulteration of EVOO is a priori unknown, the estimation of a unique concentration of ROO and ROPO simultaneously is recommended. With this objective, a new mathematical relation between chaotic parameters of UV−vis scans of mixtures of EVOO and ROO or ROPO and the respective concentrations of adulterating compounds of EVOO samples has been proposed. Following the aforementioned mathematical procedure, the most suitable models using individual combinations formed by 1−6 independent variables and

Table 4. Estimation of ROO and ROPO as Adulterating Agents of EVOO by Linear Regression Models

α_0	α_1	α_2	α_3	α_4	α_5	α_6	R^{2a}	MSE[a]
118.207	−98.880·RD						0.713	2.241
124.952	−21.390·R_{350}	−93.418·RD					0.826	1.396
127.283	−27.378·R_{500}	−10.776·R_{600}	−90.126·RD				0.865	1.107
84.599	−25.671·R_{500}	−9.444·R_{600}	−71.755·RD	22.415·BD			0.887	0.953
85.068	23.243·R_{400}	−35.683·R_{500}	12.465·R_{550}	−79.804·RD	20.085·BD		0.904	0.835
66.067	64.679·R_0	90.235·R_{100}	−86.884·R_{200}	22.977·R_{650}	−85.067·RD	14.541·BD	0.907	0.831

[a] $[\text{adulterated oil}] = \sum_{i=0}^{6} \alpha_i$.

their statistical results are shown (**Table 4**). As expected, due to the chemical differences between ROO and ROPO, the statistical results are the poorest of all groups studied. Thus, a new model using 10 independent variables has been proposed (eq **7**; $R^2 > 0.972$, MSE < 0.350).

$$[\text{adulterated oil}] = 34.853 - 67.939 \cdot R_{100} + 157.249 \cdot R_{250} + 77.573 \cdot R_{400} + 186.653 \cdot R_{450} - 134.526 \cdot R_{500} + 59.905 \cdot R_{550} - 54.715 \cdot R_{650} - 4.570 \cdot 10^6 \cdot \text{LE} - 82.846 \cdot \text{RD} + 20.747 \cdot \text{BD} \quad (7)$$

The most accurate quantification of every adulterating oil is determined using their respective individual models (eqs **4** and **5** for ROO and ROPO, respectively).

Taking into account the impossibility of previously determining which type of adulterating agent is present, in line with the statistical results ($R^2 > 0.972$, MSE < 0.350), the model described by eq **6** is suitable to estimate simultaneously the concentrations of ROO and ROPO as adulterating compounds in EVOO samples (see **Figure 3**).

External Validation of the Global Model. To validate the model described by eq **7**, a new database has been used (vide supra). It consists of chaotic parameters calculated by 18 UV−vis scans from new samples containing EVOO and ROO or ROPO ranging between 0 and 10% (*23*). As can be seen in **Figure 4**, the adulteration of EVOO with ROO and ROPO can be detected using eq **7**. The correlation coefficients and MSE values of estimated versus real values are 0.977 and 0.965 and 0.969 and 1.117, respectively. These statistical results lead us to think that linear models based on the chaotic parameters can be used to determine on line adulteration with low-grade olive oils such as ROO and ROPO.

One of the most important specifications for detecting adulterations is the lower limit of detection. Here, using only one model (eq **7**), the lower limit of detection of adulteration during the external validation process was 0.6 and 1.4% w/w for refined olive oil and refined olive−pomace oil concentrations, respectively. These values are less than for other models, such as nuclear magnetic resonance spectroscopy (NMR)/multivariate statistical analysis (5% w/w (*26*)) or the synchronous fluorescence method/partial least-squares regression (2.6% w/w (*27*)). Given the simplicity of the analytical equipment used here in comparison with the NMR apparatus, this difference in the lower limit of detection shows the power of chaotic parameters concerning adulteration. This widens the horizon to design tools which solve the problem of illegal adulterant processes, which in some cases can cause serious health damage in addition to economic fraud (*1*).

In light of these results, this is a reliable tool when the detection of ROO and ROPO concentrations of less than 10% is required. Therefore, it is suitable not only to detect adulterations but also to measure impurities when high-grade olive oil is transferred to other storage tanks that had contained lower grade olive oils and were not adequately prepared. In the latter application, given that the nature of the impurity is known, a specific model can be used (eq **5** or **6** for ROO or ROPO, respectively). In the statistical field these chaotic parameters, which can be calculated easily, extract the essential information from huge databases such as UV−vis scans.

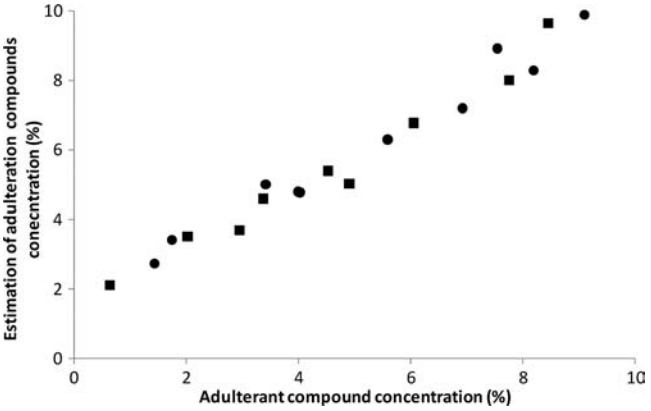

Figure 4. Experimental values from external validation samples versus their respective estimated values calculated by eq **7**: (■) **ROO;** (●) **ROPO.**

As a confirmation of the report by Devaney, this paper makes apparent the importance of using two different nature algorithms to model the chaotic behavior of a system, viz. chaotic dynamics, which studies the disordered movement of objects and fractal geometrics that analyze static images of the UV−vis scans of adulterated samples of EVOO (*21*).

The detection of refined olive oil and refined olive−pomace oil as adulterating compounds of EVOO samples represents the first step in the design of a more general tool which can detect even more adulterating agents simultaneously.

ACKNOWLEDGMENT

We thank Claudia Mignon and Carlos Calvo for their contribution to this work.

LITERATURE CITED

(1) Torrecilla, J. S. *The Olive−Its Processing and Waste Management*; Nova Publishers: New York, 2010.

(2) Mildner-Szkudlarz, S.; Jelen, H. H. The potential of different techniques for volatile compounds analysis coupled with PCA for the detection of the adulteration of olive oil with hazelnut oil. *Food Chem.* **2008**, *110*, 751–761.

(3) Peña, F.; Cárdenas, S.; Gallego, M.; Valcárcel, M. Direct olive oil authentication: Detection of adulteration of olive oil with hazelnut oil by direct coupling of headspace and mass spectrometry, and multivariate regression techniques. *J. Chromatogr. A* **2005**, *1074*, 215–221.

(4) Dourtoglou, V. G.; Dourtoglou, T.; Antonopoulos, A.; Stefanou, E.; Lalas, S.; Poulos, C. Detection of olive oil adulteration using

principal component analysis Applied on Total and Regio FA Content. *J. Am. Oil Chem. Soc.* **2003**, *80*, 203–208.
(5) Torrecilla, J. S.; Rojo, E.; Oliet, M.; Domínguez, J. C.; Rodríguez, F. Self-organizing maps and learning vector quantization networks as tools to identify vegetable oils. *J. Agric. Food Chem.* **2009**, *57*, 2763–2769.
(6) Marini, F.; Balestrieri, F.; Bucci, R.; Magrì, A. D.; Magrì, A. L.; Marini, D. Supervised pattern recognition to authenticate Italian extra virgin olive oil varieties. *Chemometrics Intell. Lab. Syst.* **2004**, *73*, 85–93.
(7) Commission Regulation (EC) No 1989/2003 of 6 November 2003 amending Regulation (EEC) No 2568/91 on the characteristics of olive oil and olive−pomace oil and on the relevant methods of analysis.
(8) Food and Agriculture organization of the United Nations. Codex alimentarius commission. Codex Standard for named vegetable oils. CODEX Stan 210, 1999 (revision and amendments: 2003, 2005).
(9) Vigli, G.; Philippidis, A.; Spyros, A.; Dais, P. Classification of Edible Oils by Employing ^{31}P and ^{1}H NMR Spectroscopy in combination with multivariate statistical analysis. A proposal for the detection of seed oil adulteration in virgin olive oils. *J. Agric. Food Chem.* **2003**, *51*, 5715–5722.
(10) Baeten, V.; Hourant, P.; Morales, M. T.; Aparicio, R. Oil and fat classification by FT-Raman spectroscopy. *J. Agric. Food Chem.* **1998**, *46*, 2638–2646.
(11) Brodnjak-Voncina, D.; Kodba, Z. C.; Novic, M. Multivariate data analysis in classification of vegetable oils characterized by the content of fatty acids. *Chemometrics Intell. Lab. Syst.* **2005**, *75*, 31–43.
(12) Sayago, A.; García-González, D. L.; Morales, M. T.; Aparicio, R. Detection of the presence of refined hazelnut oil in refined olive oil by fluorescence spectroscopy. *J. Agric. Food Chem.* **2007**, *55*, 2068–2071.
(13) Rocco, A.; Fanali, S. Analysis of phytosterols in extra-virgin olive oil by nano-liquid chromatography. *J. Chromatogr. A* **2009**, doi:10.1016/j.chroma.2009.03.081
(14) Zabaras, D.; Gordon, M. H. Detection of pressed hazelnut oil in virgin olive oil by analysis of polar components: improvement and validation of the method. *Food Chem.* **2004**, *84*, 475–483.
(15) Marini, F.; Magrì, A. L.; Bucci, R.; Magrì, A. D. Use of different artificial neural networks to resolve binary blends of monocultivar Italian olive oils. *Anal. Chim. Acta* **2007**, *599*, 232–240.
(16) Torrecilla, J. S.; Rojo, E.; Domínguez, J. C.; Rodríguez, F. Chaotic parameters and their role in quantifying noise in the output signals from UV, TGA and DSC apparatus. *Talanta* **2009**, *79*, 665–668.
(17) Vayenas, D. V.; Pavlou, S. Chaotic dynamics of a microbial system of coupled food chains. *Ecol. Model.* **2001**, *136*, 285–295.
(18) Sprott, J. C. *Chaos and Time-Series Analysis*; Oxford University Press: New York, 2003.
(19) Drazin, P. G. *Nonlinear Systems*; Cambridge University Press: Cambridge, U.K., 1992.
(20) Kant, H.; Schreiber, T. *Nonlinear Time Series Analysis*; Cambridge University Press: Cambridge, U.K., 2005.
(21) Devaney, R. L. *A First Course in Dynamical Systems, Theory and Experiments*; Addison Wesley: New York, 1992.
(22) Véhel, J. L. http://complex.futurs.inria.fr/FracLab/manual.html. **2009**.
(23) Guidance Document on the Validation of (Quantitative) Structure Activity Relationship [(Q)SAR] Models, No. 69, OECD, Series on Testing and Assessment, Organisation of Economic Cooperation and Development, Paris, France, 2007.
(24) NIST/SEMATECH e-Handbook of Statistical Methods, http://www.itl.nist.gov/div898/handbook, **2008**.
(25) Torrecilla, J. S.; Palomar, J.; García, J.; Rojo, E.; Rodríguez, F. Modeling of carbon dioxide solubility in Ionic liquids at sub and supercritical conditions by neural networks and mathematical regressions. *Chemometrics Intell. Lab. Syst.* **2008**, *93*, 149–159.
(26) Fragaki, G.; Spyros, A.; Siragakis, G.; Salivaras, E.; Dais, P. Detection of Extra Virgin Olive Oil Adulteration with Lampante Olive Oil and Refined Olive Oil Using Nuclear Magnetic Resonance Spectroscopy and Multivariate Statistical Analysis. *J. Agric. Food Chem.* **2005**, *53*, 2810–2816.
(27) Poulli, K. I.; Mousdis, G. A.; Georgiou, C. A. Rapid synchronous fluorescence method for virgin olive oil adulteration assessment. *Food Chem.* **2007**, *105*, 369–375.

Received for review September 18, 2009. Revised manuscript received December 22, 2009. Accepted December 28, 2009.